CHAPTER VI
HYBRID POLYBENZOXAZINE COMPOSITE MEMBRANE FOR CO_2/CH_4 SEPARATION

6.1 Abstract

By combining the advantages of both matrix and filler to improve the gas separation performance, a novel mixed matrix membrane (MMM), polybenzoxazine-ZSM-5, has been successfully fabricated. The SEM micrographs revealed good interfacial adhesion between polybenzoxazine and ZSM-5 particles since no micron size void was observed. The XRD pattern showed no change in the crystal structure of the ZSM-5 after mixing with the polymer matrix. By using a single-gas measurement, it was found that the CO_2 and CH_4 permeability of MMM was decreased, while the CO_2/CH_4 selectivity was increased with an increase in the zeolite loading. The 5 wt.% of ZSM-5 loading showed great CO_2 and CH_4 permeability and selectivity when compared with those with highest % of ZSM-5 loading content.

Keywords: Mixed matrix membrane (MMM), Polybenzoxazine, ZSM-5, Gas separation

6.2 Introduction

Normally, the types of gas presenting in the natural gas are H_2, N_2, O_2, CH_4 and CO_2, which are independent sources of the synthesis gas production. However, one problem commonly found in the natural gas processing is the pipeline corrosion, which is induced by the acidic gas such as acidic carbon dioxide gas, etc. To reduce the pipeline corrosion and also to produce high-purity energy products, gas separation technique by membrane is an attractive approach to separate carbon dioxide gas (longer and slender molecule) from methane (more compact molecule with slightly longer cross-section) in the natural gas processing because it requires low energy consumption, simple operation and low maintenance [1].

One of the most important elements in gas separation technique is the membrane. In this study, polybenzoxazine, which is a high performance thermosetting resin, was selected as the membrane matrix. Polybenzoxazine exhibits excellent properties such as low shrinkage after curing, low water absorption, good thermal stability and high glass transition temperature [2-4]. However, in order to improve the selectivity of a dense membrane in the separation process, zeolite — which can act as a molecular sieve — was added to form a mixed matrix membrane (MMM) or composite membrane to enhance the separation performance, while still maintaining low cost, simplicity of operation and great processing flexibility.

The purpose of this work was to develop a new MMM by using polybenzoxazine as the continuous phase for gas separation and to study the ability of this MMM for the separation of carbon dioxide gas from methane.

6.3 Experimental

6.3.1 Materials

Bisphenol-A (BPA, $C_{15}H_{16}O_2$) and 1,6-Hexadiamine (hda, $C_6H_{16}N_2$) were purchased from Aldrich, Germany. Formaldehyde (CH_2O, analytical grade) was purchased from Merck, Germany. 1,4-Dioxane ($C_4H_8O_2$, analytical grade) was purchased from Labscan, Ireland. All chemicals were used without further purification. Zeolite ammonium (ZSM–5) powder — Si/Al ratio is 24.3, the median

particle size is 4.5 μm, and surface area is 450 m^2/g — was purchased from Zeolyst International, USA. In order to remove the adsorbed water vapor or other organic vapors, zeolite was dehydrated at 250° C for 2 hours under vacuum before use.

6.3.2 Measurements

The structural characteristics of benzoxazine precursor were measured using Fourier Transform Infrared Spectrometer (FT-IR) obtained from a Thermo Nicolet and Proton Nuclear Magnetic Resonance (^{1}H NMR) which were recorded on a Varian Mercury 300 (300 MHz) instrument. For ^{1}H NMR experiment, benzoxazine precursor was dissolved in deuterated chloroform ($CDCl_3$) for 24 hours prior to use. Attenuated Total Reflectance Infrared Spectrometer (ATR-IR) spectra of polybenzoxazine membranes were obtained from a Thermo Nicolet by using ZnSe 45° (flat plate) with a scanning resolution of 4 cm^{-1}. The interaction between the gas molecule and the MMM was also studied from a Thermo Nicolet by using gas cell holder. The membrane morphology was investigated by using Scanning Electron Microscopy (SEM) (FE-SEM S4800). X-Ray Diffractometer (XRD) was used to study the XRD patterns of zeolite ZSM–5 before and after added into polybenzoxazine matrix.

6.3.2.1 Gas permeability apparatus

In this study, CO_2 (Prax Air) and CH_4 (TIG) were used as testing gases for all membranes. All tested gases were of a high purity (HP) grade and used as received. A schematic diagram of the system used to carry out the gas permeability experiments and the experimental setup including gas sources, a membrane testing unit and a bubble flow meter is shown in Figure 6.1. The experiments were a conducted at room temperature under a pressure of 20 psi.

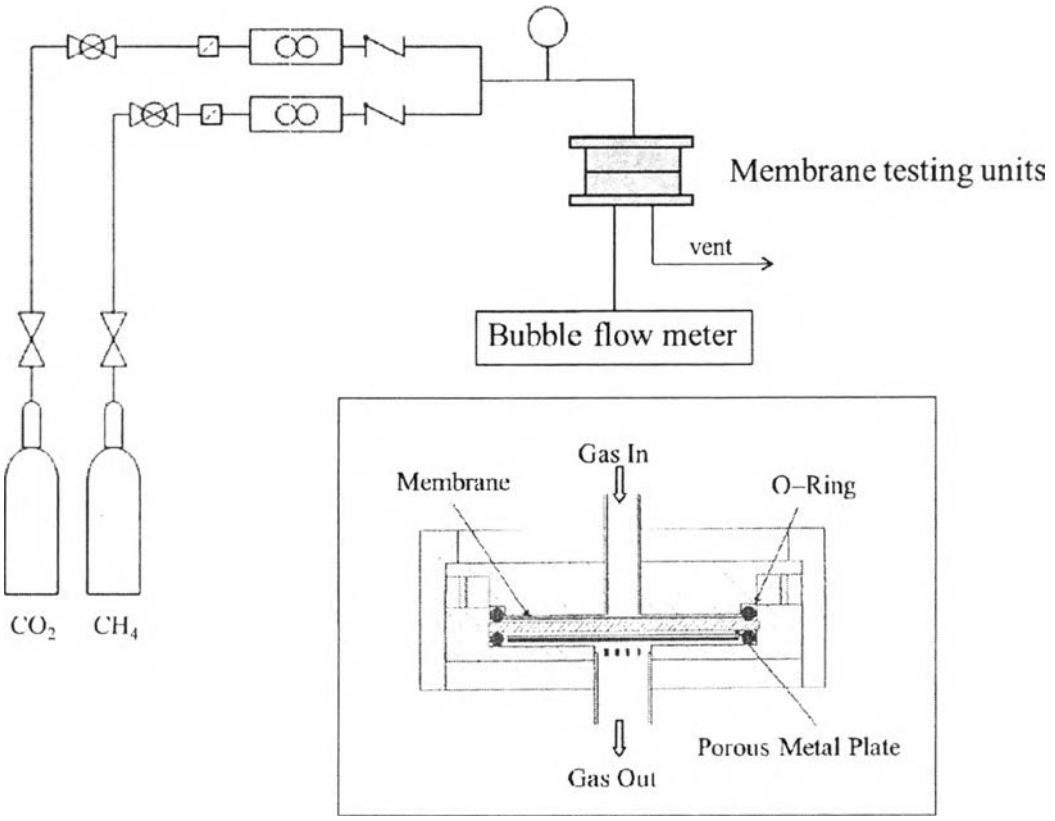

Figure 6.1 Experimental setup for a gas permeability apparatus and schematic diagram of the membrane testing unit.

6.3.3 Methodology

6.3.3.1 *Synthesis of Polybenzoxazine Precursors*

The polybenzoxazine precursor was synthesized by using bisphenol-A (BPA, $C_{15}H_{16}O_2$), formaldehyde (CH_2O) and 1,6-hexadiamine (hda, $C_6H_{16}N_2$), with a molar ratio of 1:4:1, respectively [4,5]. First, BPA (6.84 g) was dissolved in a 1,4-dioxane (15 ml) in a 50 ml glass bottle and stirred until the clear solution was obtained. Formaldehyde solution (9.73 g) was then added into the PBA solution. The reaction was cooled with an ice bath. After that hda (3.48 g) was added dropwise into the mixture and stirred continuously until clear yellowish liquid was obtained. Scheme 6.1 depicts the synthesis process of benzoxazine precursor.

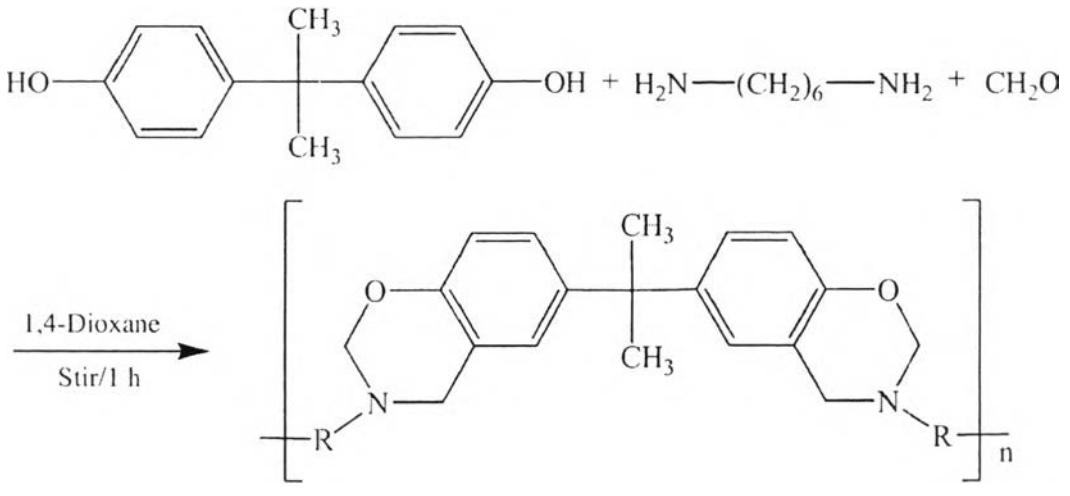

Scheme 6.1 The synthesis of benzoxazine precursor.

6.3.3.2 *Preparation of Polybenzoxazine Membranes*

The benzoxazine precursor obtained from the reactions was heated and stirred continuously until viscous liquid was obtained. Then the mixture was left to cool down to room temperature and then cast on a glass plate which was wrapped with aluminum foil with a thickness of approximately 300 μm using Elcometer 3580 casting knife film applicator (from elcometer/inspection equipment). The membrane was dried at room temperature in air for one day yielding a self-standing yellowish transparent membrane. The membrane was then placed in an air-circulating oven at 120 °C for 24 hours. The thickness of the obtained membrane was around 150±10 μm.

6.3.3.3 *Preparation of Mixed Matrix Membranes (MMMs)*

Various contents of ZSM–5 were dispersed in 1,4-Dioxane and stirred for 3 hours. After that, the mixture was sonicated for 10 min to improve the dispersion of zeolite particles in the solution. Zeolite particles were then "primed" by adding approximately 15 wt. % of total amount of polybenzoxazine, to increase the compatibility between zeolite and polymer and to minimize the aggregation of zeolite particles. The mixture was then stirred by using a magnetic stirrer to enhance the homogeneity. After the remaining polybenzoxazine was added, the final mixture

was further stirred continuously for 2 hours before use. The concentrations of zeolite in polybenzoxazine were varied from 1 wt.%, 5wt.% and 10wt.%.

6.3.3.4 *Gas Permeation Measurements*

The single-component gas permeation (CH_4 and CO_2) experiments of polybenzoxazine membrane and polybenzoxazine–ZSM–5 membranes (MMMs) were carried out at 25° C in sequences by using a gas permeation testing unit in which the membrane was placed on a porous metal plate, then the two compartments were fixed together to prohibit the leakage. The area of the membrane in contact with the gas was 44.17 cm^2. The pressure difference across the membrane was maintained at 20 psi. Once reached the steady–state, individual gas flow rates were measured using a soap bubble flow meter. The attained data were used to calculate the gas selectivity and permeability. The ideal separation factor (Gas Selectivity, $S_{A/B}$) for component A and B is defined as the ratio of each component as shown in equation 6.1:

$$S_{A/B} = \frac{P_A}{P_B} \quad , \tag{6.1}$$

The permeability coefficient for the permeated gas can be obtained by equation 2:

$$\left(\frac{P}{\delta}\right)_i = \frac{Q_i \times 14.7 \times 10^6}{(A) \times (\Delta P) \times 76} \quad , \tag{6.2}$$

where

$\left(\frac{P}{\delta}\right)_i$ = permeance of gas 'i' (GPU),

P = permeability of gas 'i' (10^{-10} cm^3 (STP) cm/cm^2 s cm Hg)
(1 Barrer = 10^{-10} cm^3 (STP) cm/cm^2 s cm Hg = 7.5×10^{-18} m^2 s^{-1} Pa^{-1}),

δ = thickness of membrane (μm),

Q_i = volumetric flow rate of gas 'i' (cm^3/sec),

A = membrane area (cm^2), and

ΔP = pressure difference between the feed side and the permeating side (psi).

6.4 Results and Discussion

6.4.1 Polybenzoxazine Membrane Characterizations

Benzoxazine precursor, Poly(BA-hda), was derived from the reaction of PBA, hda and formaldehyde at a molar ratio of 1:4:1 via a "quasi-solventless" method in which a small amount of dioxane was used only to facilitate the mixing of the reactants. The ^{1}H NMR measurement was conducted to confirm the synthesis process. ^{1}H NMR spectra (Figure 6.2) is in agreement with the work reported by Takeichi *et al.* (2005) [7]. The results showed that the obtained precursor was partially cured benzoxazine as confirmed by the characteristic peaks of Poly(BA-hda) assigned to the methylene protons of O–CH_2–N (a) and Ar–CH_2–N (b) of oxazine ring observed at around 4.80 and 3.90 ppm, respectively and the methyl protons of bisphenol-A (d) and methylene protons of opened-ring polybenzoxazine (c) observed at 1.57 and 2.85 ppm, respectively. The appearance and SEM micrographs of polybenzoxazine (Figure 6.3a, 6.3b, 6.4a and 6.4b) reveal that the obtained Poly(BA-hda) was a dense membrane.

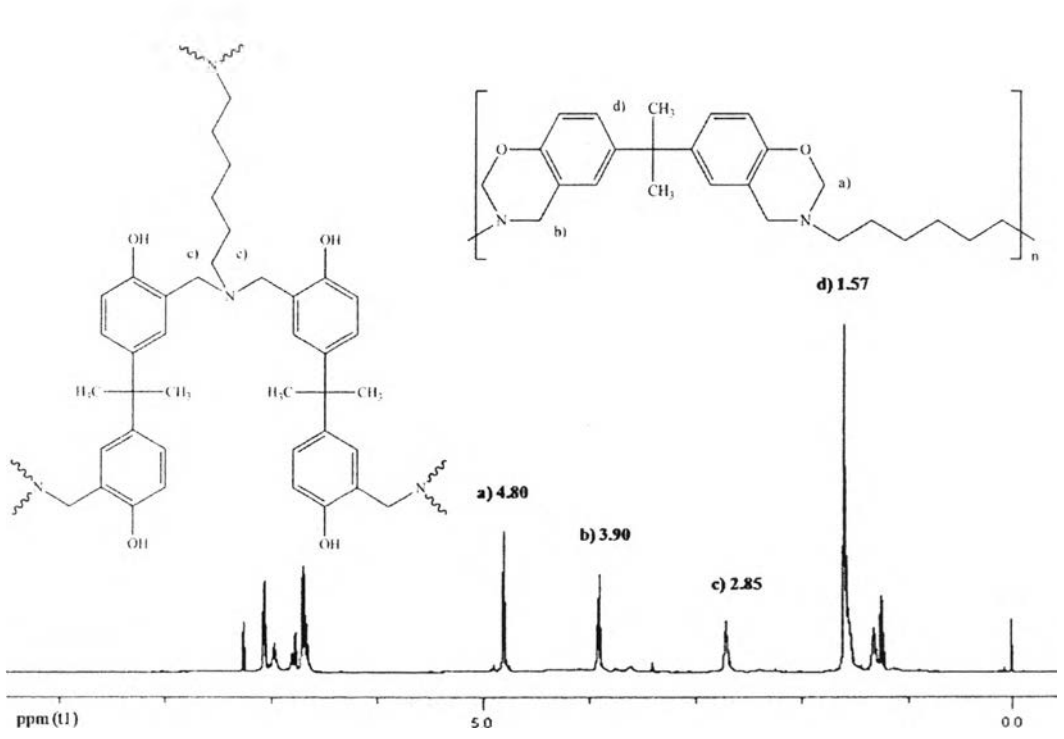

Figure 6.2 ^{1}H NMR spectra of polybenzoxazine precursors: Poly(BA–hda).

6.4.2 Characterization of Mixed Matrix Membranes (MMMs)

Formation of Mixed Matrix Membranes was prepared by adding various contents of ZSM–5 (1 wt.%, 5wt.% and 10 wt.%) into the polybenzoxazine solution and cast on glass plates. The membranes were dried at 120° C for 24 hours yielding the mixed matrix membranes (MMMs) with the thickness around 150±10 μm and a testing diameter of 7.5 cm for the permeability measurements. The characteristics of partially cured mixed matrix membranes are shown in Figure 6.3c and 6.3d. Even after ZSM–5 was added as a filler, the resulting MMM was still flexible (Figure 6.3d). The MMMs with different zeolite loadings were examined by SEM to determine that the zeolite ZSM–5 particles were homogeneously distributed in polybenzoxazine membrane matrix without forming any large agglomerate as shown in figure 6.4c, 6.4e, and 6.4g.

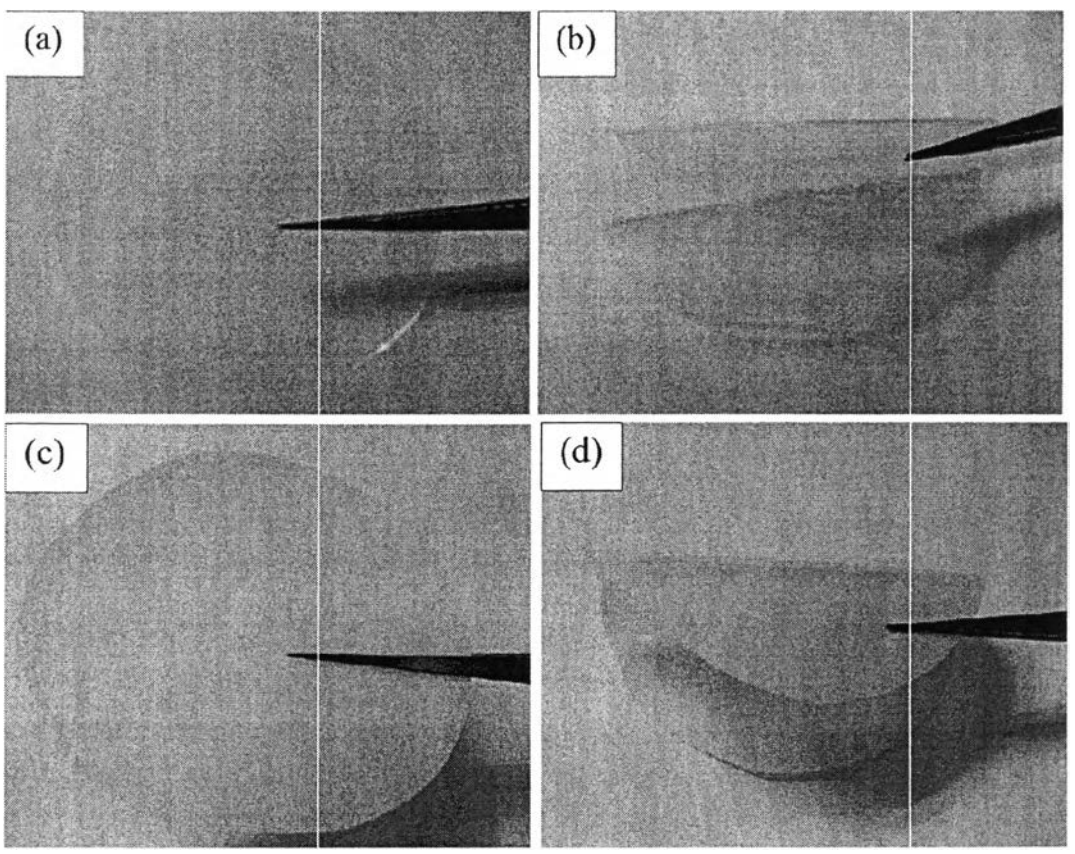

Figure 6.3 Appearance of polybenzoxazine membrane: Poly(BA–hda) and mixed matrix membranes: Poly(BA–hda)–ZSM–5 MMMs.

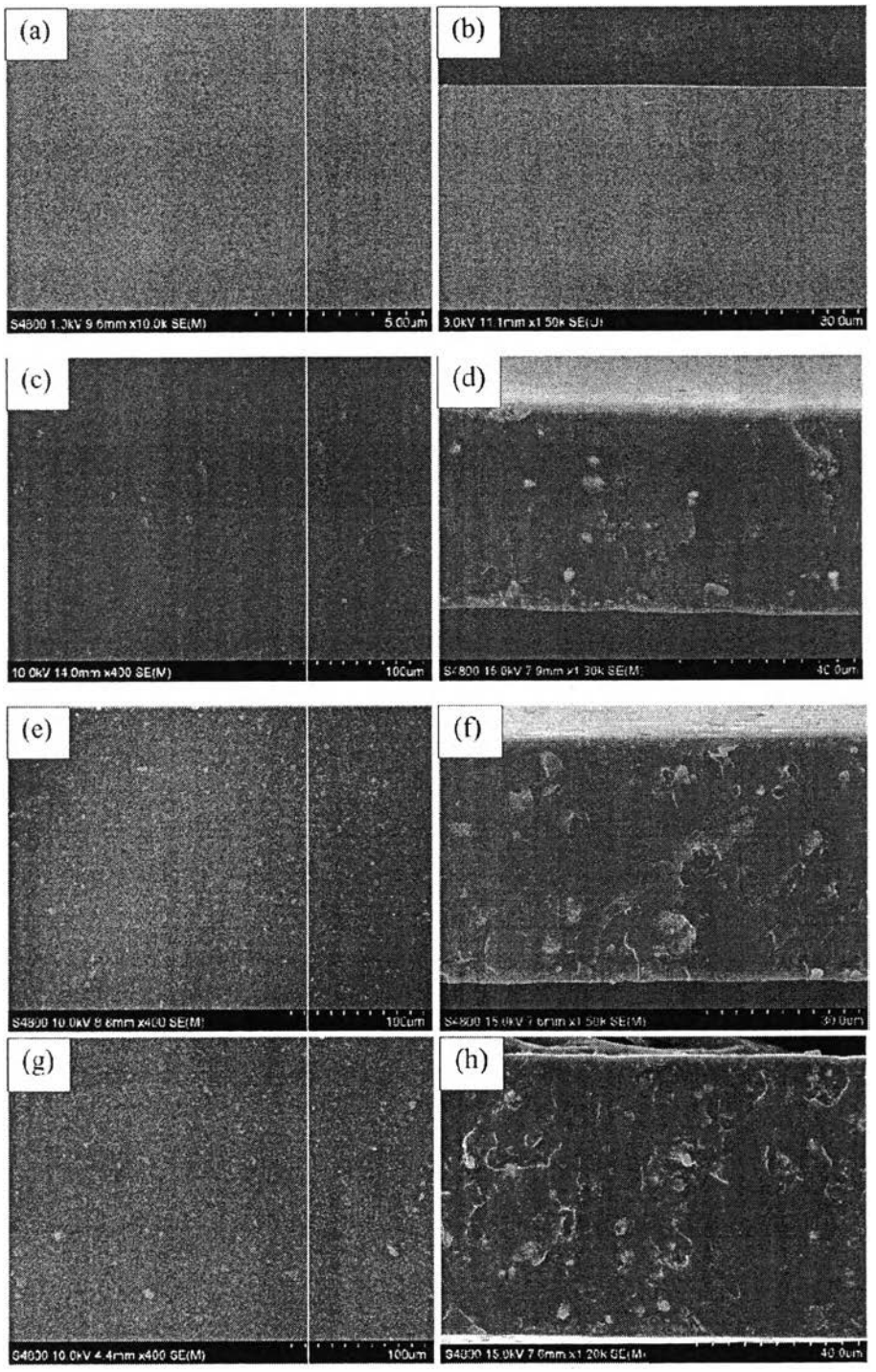

Figure 6.4 SEM micrographs of surface and cross-section of Poly(BA–hda) membrane: (a) and (b), and poly(BA-hda)–ZSM–5 MMMs with 1 (c) and (d), 5 (e) and (f), and 10 wt. % (g) and (h) of ZSM–5 loadings.

The SEM micrographs are shown in Figure 6.4d, 6.4f and 6.4h for the cross–section morphology of polybenzoxazine membrane filled with different zeolite loadings, where the cubic particles are zeolite ZSM–5 crystals, and the continuous phase is polybenzoxazine. At the interface between the polymer and ZSM–5 particles, there is no micron size void suggesting that the contact between the polymer and the ZSM–5 particles is good which might be due to the chemical interaction between the ZSM–5 particles and the polybenzoxazine. Further investigation will be discussed later.

The XRD patterns for ZSM–5 and MMMs are shown in Figure 6.5. The XRD pattern of MMMs shows the presence of all major peaks for ZSM–5 zeolite similar to that of the ZSM–5 reference pattern given by the JCPDS (Joint Committee on Powder Diffraction Standards) indicating that ZSM–5 zeolite existed in the MMMs.

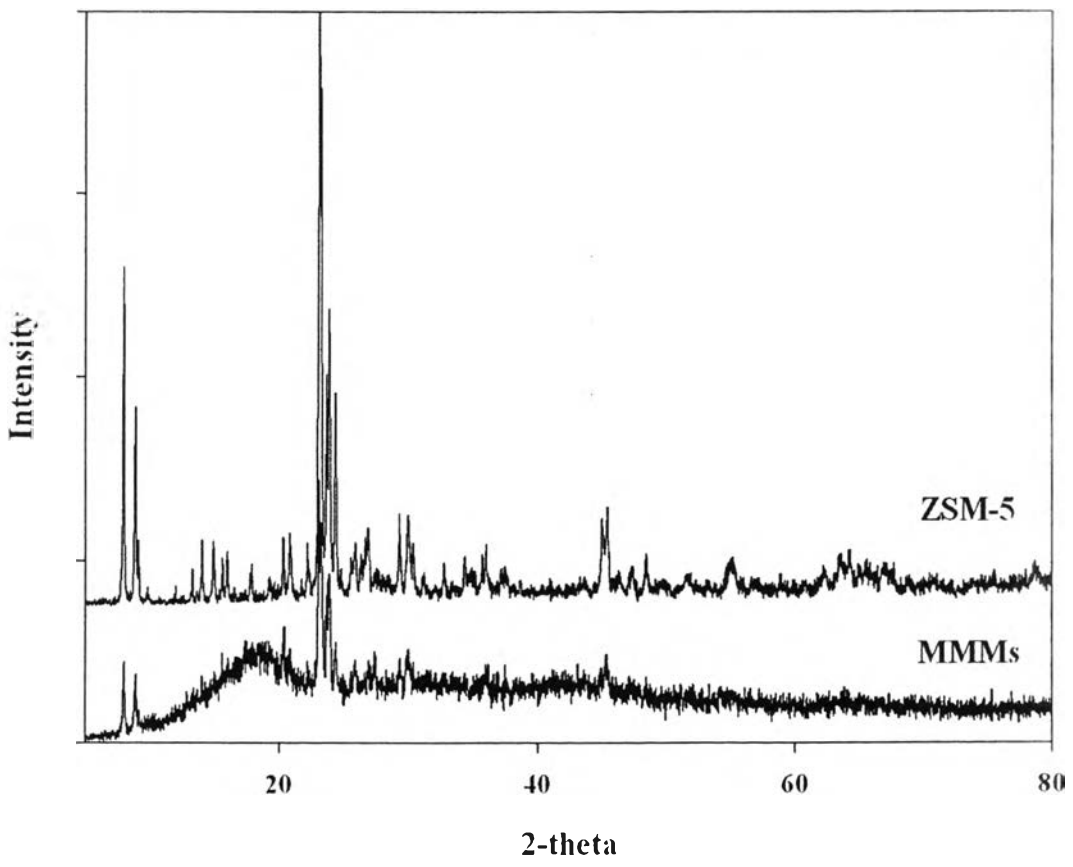

Figure 6.5 XRD patterns of ZSM–5 and MMMs.

6.4.3 Interfacial interaction of ZSM–5 and polybenzoxazine (PBZ)

The FT-IR spectra of ZSM–5, polybenzoxazine and MMMs are shown in Figure 6.6. According to Mohamed *et al.* [8] as studied in 2005, ZSM–5 showed the bands near 1219 and 542 cm^{-1} corresponding to the characteristics of double five membered ring, 1080 cm^{-1} represented the internal asymmetric stretching vibration of Si–O–T linkage (T represents Si or Al), while the peak at 790 cm^{-1} was attributed to the symmetric stretching of the external linkage. The peak at 450 cm^{-1} represented the T–O bending vibration of the SiO_4 and AlO_4 internal tetrahedral and the bands around 542 and 450 cm^{-1} were the characteristic peaks of the ZSM–5 crystalline structure.

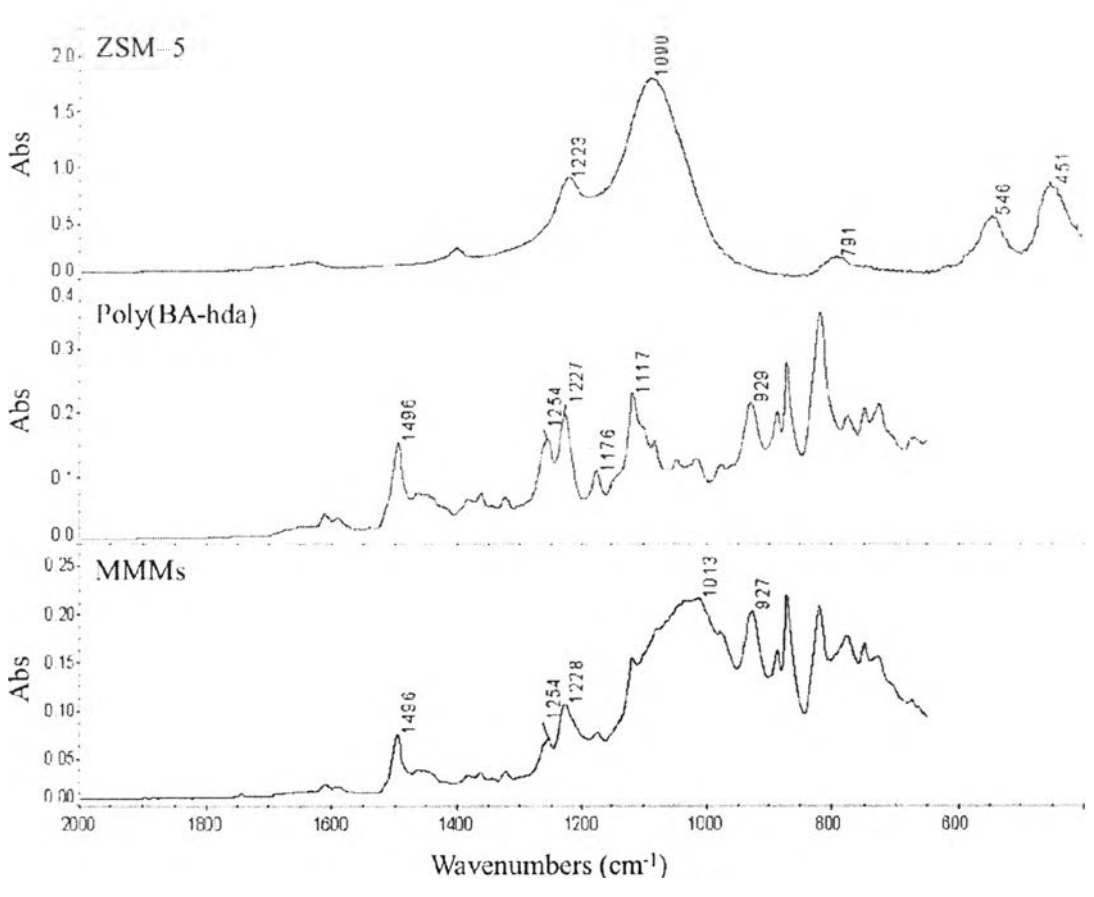

Figure 6.6 The FT-IR spectra of ZSM–5, Poly(BA–hda) and MMMs.

The FT-IR of poly(BA-hda) are also shown in Figure 6.6. The asymmetric stretching of C–O–C (1227 cm^{-1}), the asymmetric stretching of C–N–C (1176 cm^{-1}), and CH_2 wagging of oxazine (1254 cm^{-1}) were observed. Additionally, the characteristic absorptions assigned to trisubstituted benzene ring at 1496 cm^{-1} and the out-of-plane bending vibrations of C–H at 929 cm^{-1} were observed, indicating that precursors contained benzoxazine functionality [7].

Poly(BA-hda)–ZSM–5 showed the peak at 1013 cm^{-1} attibuted to Si–O–C and the broadening peak observed around 1117 cm^{-1} represented the C–OH group of poly(BA-hda) suggesting that ZSM–5 interated with poly(BA-hda). The chemical structures of ZSM–5 and poly(BA-hda) are shown in Scheme 6.2.

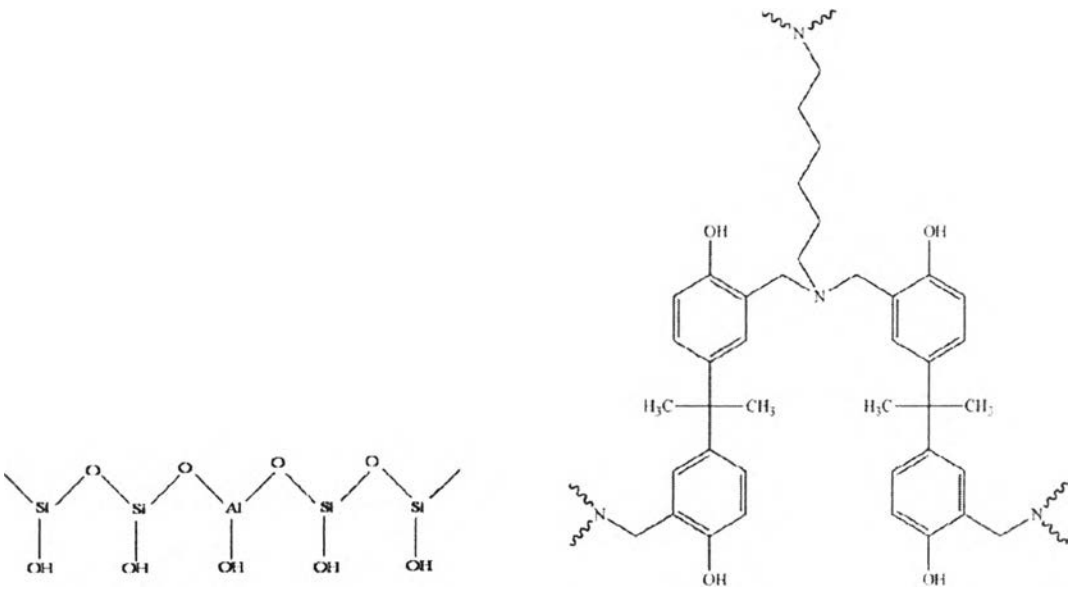

a) ZSM–5 b) Poly(BA-hda)

Scheme 6.2 Chemical structures of ZSM–5 (a) and Poly(BA-hda) (b).

6.4.4 Gas Permeability

Polybenzoxazine membrane and MMMs were tested by using the single gas measurement. The permeability and selectivity of CO_2 and CH_4 in polybenzoxazine membranes and mixed matrix membrane are depicted in Figure 6.7a and 6.7b.

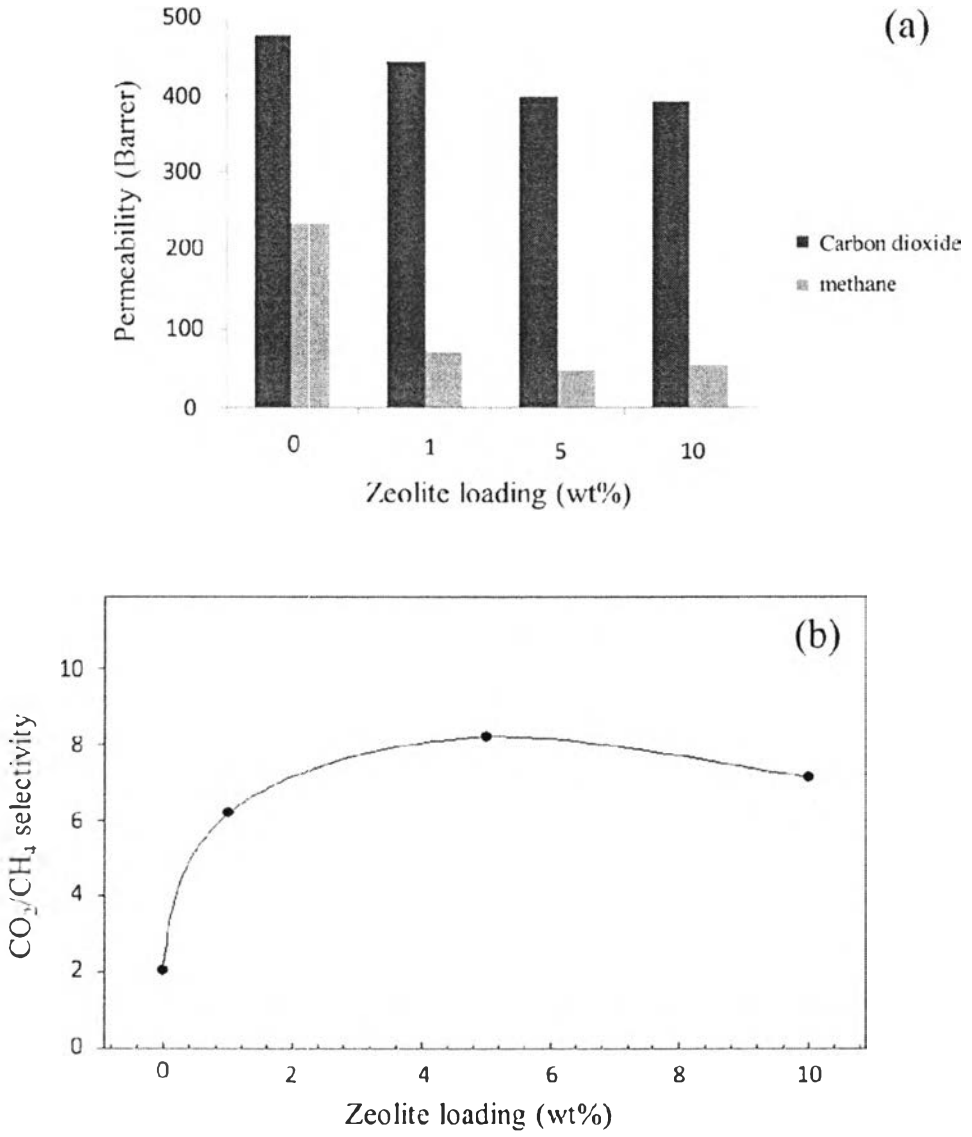

Figure 6.7 Effect of ZSM–5 loading on CO_2 and CH_4 permeability and selectivity.

6.4.4.1 The effect of zeolite loading on the CO_2 and CH_4 permeability

The CO_2 and CH_4 permeability of MMMs were decreased with increasing zeolite contents. The addition of ZSM–5 into poly(BA-hda) polymer matrix resulted in the drop-off CO_2 and CH_4 permeability comparing with compare those of the pure poly(BA-hda) membrane (Figure 6.7a). This might be due to zeolite particle disturbed the transient gap of polymer chains. Generally, the transient gap allowed penetrant molecules to pass through polymer matrix. The presence of zeolite obstructed the movement of the polymer chains and reduced polymer chain mobility

[9]. As a result, it was more difficult for, CO_2 and CH_4 molecules to penetrate through the membranes.

For poly(BA-hda), the gas permeability decreased significantly as the penetrant size increased. In conventional glassy polymers, the size of gas molecules showed more significant effect on diffusion rather than on solubility, leading to a dramatic decrease in permeability as the size of the gas molecules increased [10]. From the results, the membranes were selective to CO_2 because CO_2 preferentially adsorbed on to the membranes [11]. The molecular kinetic diameters of CO_2 and CH_4 are 3.3 Å and 3.8 Å, respectively [12]. From a view point of the configurational diffusion, even a small difference in molecular size between CO_2 and CH_4 causes a big difference in the rate of diffusion through the ZSM–5 zeolite channels. Therefore, the diffusion of CO_2 is faster than that of CH_4 [11]. Subsequently, CO_2 and CH_4 can be separated by polybenzoxazine–ZSM–5 zeolite mixed matrix membrane. However, as ZSM–5 loadings were increased, CO_2 and CH_4 permeability was not enhanced. This is because the pore opening of zeolite ZSM–5 (5 Å) was larger than kinetic diameters of both CO_2 and CH_4 molecules. Thus, allowing both gases to freely pass through the membrane.

6.4.4.2 *The effect of zeolite loading content on the CO_2/CH_4 selectivity*

The CO_2/CH_4 selectivity for ZSM–5 at different loadings is shown in Figure 6.7b. At the beginning, the CO_2/CH_4 selectivity increased with an increase in the zeolite loadings. After that the increasing of ZSM–5 into the membrane did not enhance CO_2/CH_4 selectivity. This is due to its large pore opening compared to kinetic diameter of CO_2 and CH_4 molecules, or molecular sieving mechanism of ZSM–5 plays a minor role in CO_2/CH_4 separation [7]. Compared with the polybenzoxazine membrane, those MMMs showed better CO_2/CH_4 selectivity, the CO_2/CH_4 selectivity for 0 wt.%, 1 wt.%, 5 wt.% and 10 wt.% of zeolite loading were 2.04, 6.19, 8.21 and 7.12, respectively, suggesting that ZSM–5 zeolite improved the selectivity for CO_2 and CH_4 separation. To make the gas separation process economically attractive, the 5 wt.% of zeolite loading showed the highest CO_2 and CH_4 selectivity and great CO_2/CH_4 permeability when compared with those with higher % of ZSM–5 loading content; thus, the MMM with 5 wt.% of zeolite was chosen for further investigation.

Since the Si/Al ratio of zeolite ZSM–5 is 23, the substitution of a silicon atom for an aluminium atom cause the electric field gradients which form strong interaction with the permanent electric quadrupole moment of CO_2 molecules [13] and are able to selectively attract CO_2 molecules than CH_4 molecules resulting in obstructing other CO_2 molecules to pass freely through the MMMs. Even though the pore size of ZSM–5 is around 5 Å which is larger than the kinetic diameters of both CO_2 (3.3 Å) and CH_4 (3.8 Å) molecules. Thus, the gas separation performance not only depends on the pore size but also the interaction between gas molecules and MMMs.

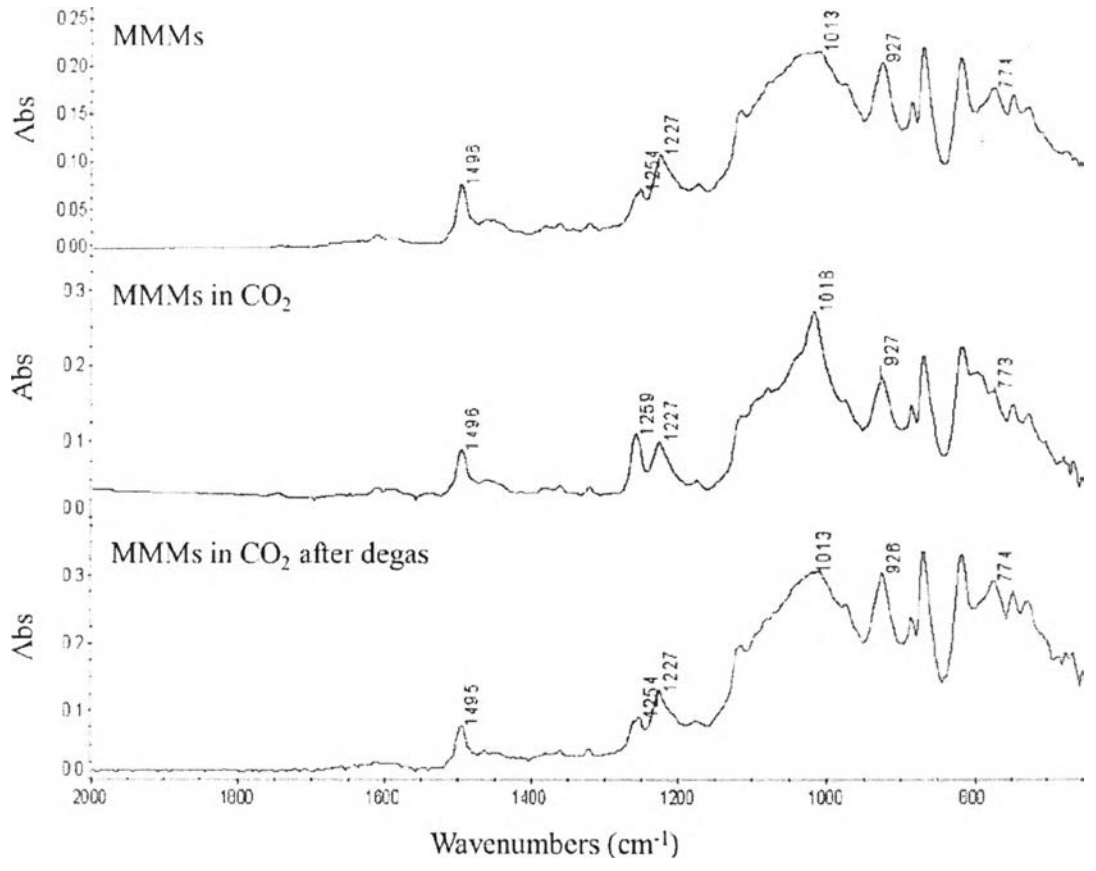

Figure 6.8 The FT-IR spectra of MMMs in CO_2 and after degas.

6.4.5 The interaction between penetrated gas and mixed matrix membrane

In general, CO_2 has higher permeation rate than CH_4. The presence of certain functional groups in the polymer backbone may enhance or depress the permeation of certain gas over another as a result of some interactions between the gas molecules and those functional groups [14]. Figure 6.8 shows the FT-IR spectra of MMMs containing adsorbed CO_2 and after degas. The intensity of the C–O–C band at 1254 cm^{-1} increased when CO_2 was purged into the system. The shape of the band at 1013 cm^{-1} (Si–O–T) changed and shifted to higher frequency (1018 cm^{-1}) and the peak at 774 cm^{-1} disappeared. However, after degassing, the FT-IR spectrum revealed the same pattern and intensity as that of the original MMMs suggesting that CO_2 was absent in MMMs. Thus the adsorption of CO_2 on to MMMs was a reversible process and the interaction CO_2 molecule and MMMs was unstable.

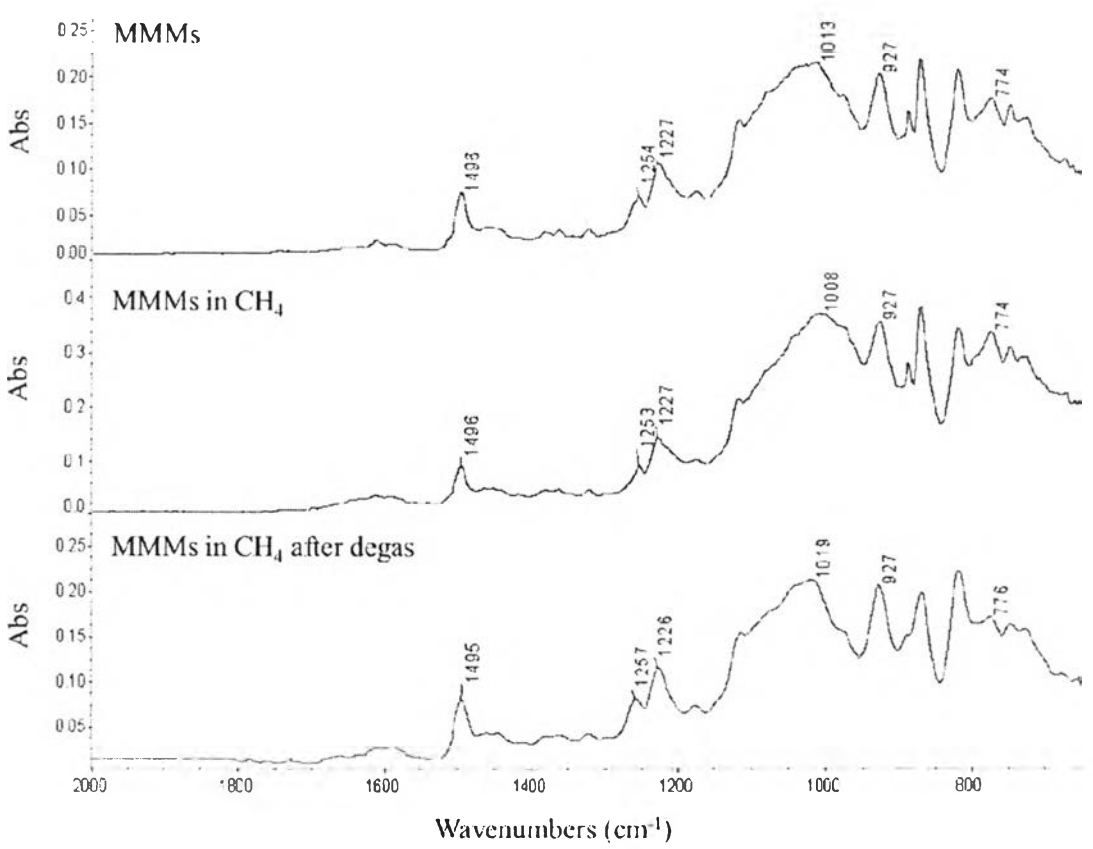

Figure 6.9 The FT-IR spectra of MMMs in CH_4 and after degas.

Figure 6.9 shows the FT-IR spectra of MMMs in the environment containing CH_4 and after degas. The shape of the band at 1013 cm^{-1} (Si–O–T) changed and shifted to lower frequency (1008 cm^{-1}). However, after degassing, the IR spectrum showed the same pattern and intensity as that of original MMMs. This also suggests that the interaction between CH_4 molecule and MMMs was reversible.

6.4.6 Comparison of gas separation performance

The CO_2/CH_4 selectivity of poly(BA-hda)–ZSM–5 was compared with previous works as show in Table 6.1. Our result show better performance than the other membranes due to the polybenzoxazine–ZSM–5 membrane and comfortable condition.

Table 6.1 Performance of the polymer membranes in CO_2/CH_4 separation

Membrane	CO_2/CH_4 Selectivity	Reference
PDMS	3.5	[15]
Poly(St-co-MAH-graft-DMS)	4.0	[15]
Activated carbon fibers	5.2	[16]
Na–X membrane	3.5	[17]
Poly(BA-hda)–5%ZSM–5	8.21	this work

6.5 Conclusions

Mixed matrix membranes, polybenzoxazine–ZSM–5, were successfully synthesized from bisphenol-A, formaldehyde and 1,6-hexadiamine. The 5 wt.% of ZSM–5 loading showed the highest CO_2 and CH_4 selectivity and great CO_2/CH_4 permeability when compared with those with higher percent of ZSM–5 loading content. Increasing the zeolite loading did not significantly improve neither gas permeability nor CO_2/CH_4 selectivity.

6.6 Acknowledgements

We are grateful for the scholarship and funding of this research work provided by the Petroleum and Petrochemical College; The Nation Center of excellence for Petroleum, Petrochemicals, and Advanced Materials; the Ratchadapisake Sompote Fund, Chulalongkorn University, the Thailand Research Fund (TRF); the National Science and Technology Development Agency (NSTDA); and, The Development and Promotion of Science and Technology Talents project (DPST). Additionally, the authors would like to thank Assistant Professor Dr. Apanee Luengnaruemitchai and Associate Professor Dr. Therasak Rirksomboon for gas separation equipment.

6.7 References

[1] D. Şen, H. Kalıpçılar, L. Yilmaz, J. Membr. Sci. 303 (2007) 194.

[2] X. Ning, H. Ishida, J. Polym. Sci. 32, (1994) 1121.

[3] T. Agag, T. Takeichi, J. Polym. Sci. Part A: Polym. Chem. 45 (2006) 1878.

[4] T. Chaisuwan, H. Ishida, J. Appl. Polym. Sci. 101 (2006) 548.

[5] P. Lorjai, T. Chaisuwan, S. Wongkasemjit, J. Sol-Gel Sci. Tecnol. 52 (2009) 56.

[6] P. Lorjai, T. Chaisuwan, S. Wongkasemjit, Mater Sci. Eng., A. 527 (2009) 77.

[7] T. Takeichi, T. Kano, T. Agag, Polymer, 46 (2005) 12172.

[8] R.M. Mohamed, H.M. Aly, M.F El–Shahat, I.A. Ibrahim, Microporous Mesoporous Mater. 79 (2005) 7.

[9] H. Cong, M. Radosz, B. F. Towler, Y. Shen Sep. Purif. Technol. 55 (2007) 281.

[10] S. Thomas, I. Pinnau, M.D. Guiver, J. Membr. Sci. 333 (2009) 125.

[11] A. Corma, Chem, 95 (1995) 559.

[12] J. Zhang, J. Lu, W. Liu, Q. Thin Solid Films 340(1999) 106.

[13] S.A.S. Rezai, J. Lindmark, C. Andersson, F. Jareman, K. Moller, J. Hedlund, Microporouse Mesoporous Mater. 108 (2008) 136.

[14] F. Hamad, K.C. Khulbe, T. Matsuura, J. Membr. Sci. 186 (2001) 281.

[15] F. Suzuki, K. Nakane, Y. Hata, J. Membr. Sci. 104 (1995) 283.

[16] S.H. Moon, J.W. Shim J. Ccolloid Interface Sci. 298 (2006) 523.

[17] K. Weh, M. Noack, I. Sieber, J. Caro, Microporous Mesoporous Mater. 54 (2002) 27.